

Surface and bulk properties improvement of HDPE by a batch plasma treatment

Mintra Meemusaw, Rathanawan Magaraphan

Polymer Processing and Polymer Nanomaterials Research Unit, National Center of Excellence for Petroleum, Petrochemical, and Advanced Materials, the Petroleum and Petrochemical College, Chulalongkorn University, Bangkok 10330, Thailand

Correspondence to: R. Magaraphan (E-mail: rathanawan.k@chula.ac.th)

ABSTRACT: High-density polyethylene (HDPE) pellets were modified via atmospheric plasma treatment using nitrogen flushing. The new application of plasma treatment was introduced in this work, namely a batch treatment on plastic pellets just prior to its feeding to the extrusion process in comparison with the conventional surface treatment of the plastic sheet. The effect of treatment time (15–120 s) on wettability, chemical, thermal, and mechanical properties of the modified HDPE were investigated and compared with the typical surface-treated HDPE and untreated HDPE. The pellet treatment distributed well the hydrophilicity groups so that both surface and bulk properties were improved. It showed an enhancement of wettability similar to surface treatment at short treatment time (15 s). Attenuated total reflection-Fourier transform infrared spectroscopy and X-ray photoelectron spectroscopy revealed the presence of new chemical groups (nitrogen and oxygen up to 5 and 42 at %, respectively). In addition, crosslinked structure was also disclosed by solvent extraction (gel content of 3.5–5.5 wt % increased with treatment time) and significantly affected to decrease the crystallinity from 76% in the untreated sample to 63%. The decomposition process of the pellet treatment samples was delayed. Lastly, pellet treatment yielded advantages in remaining hydrophilicity during aging and improving mechanical properties. © 2015 Wiley Periodicals, Inc. *J. Appl. Polym. Sci.* **2016**, *133*, 43011.

KEYWORDS: polyolefins; thermal properties; X-ray

Received 30 July 2015; accepted 30 September 2015

DOI: 10.1002/app.43011

INTRODUCTION

Polyethylene (PE) is widely used in many sectors of industry due to its exceptional bulk properties. It has high processability, good chemical resistance, high impact strength, high flexibility, and relatively low cost. However, PE has low surface free energy due to its nonpolar structure. This limits PE for use in applications requiring good adhesion to polar surfaces or metal such as coating and painting.^{1–3} Plasma treatment is one of the techniques used to enhance wettability and adhesion of nonpolar polymers. It also offers a more environmental friendly path to convert hydrophobic surfaces to hydrophilic surfaces than chemical methods; hence, wettability and good adhesion of nonpolar polymers are developed.^{4–6} Atmospheric plasma for surface treatment has been available industrially for labeling or painting of PE objects. It is known for a stunning effect on introducing hydrophilicity to the low surface adhesion of polyolefins within a short time. However, the produced hydrophilicity is quite fragile and lasts in a limited time, e.g., typically within a day.

In recent years, there are several reports revealing the improvement of hydrophilicity of PE surface after plasma treatment with

different plasma gases.^{7–9} Interestingly, Arpagaus *et al.*¹⁰ reported that wettability of high-density polyethylene (HDPE) powders was improved by plasma surface modification with treatment time within less than 0.1 s using the mixed Ar–O₂ gases. They showed the reduction of water contact angle of HDPE powder from >90° for untreated sample to 65° for treated samples. In addition, the nitrogen-containing plasma is one of the plasma treatments commonly applied to polymeric membranes and polymer films because it generates many surface functionalities including amine, imine, amide, and nitrile groups.^{11–13} Bretagnol *et al.*¹¹ found that nitrogen was introduced to the hydrophobic surface of the treated samples (the nitrogen to carbon ratio, N/C, ~13%); C–N and C–O functionalities were observed on PE powder surfaces after nitrogen and ammonia plasma modification. Although the mechanism of nitrogen plasma has not been clearly investigated, the reaction was found to occur through radicals as reported by Xiao-Jing *et al.*¹⁴ They studied the radical concentration of poly(vinyl chloride) (PVC) films after the nitrogen plasma treatment by electron spin resonance (ESR) spectrometer and found that it was enhanced by 10 times compared with that of neat PVC. Unlike electron irradiation where bulk properties of

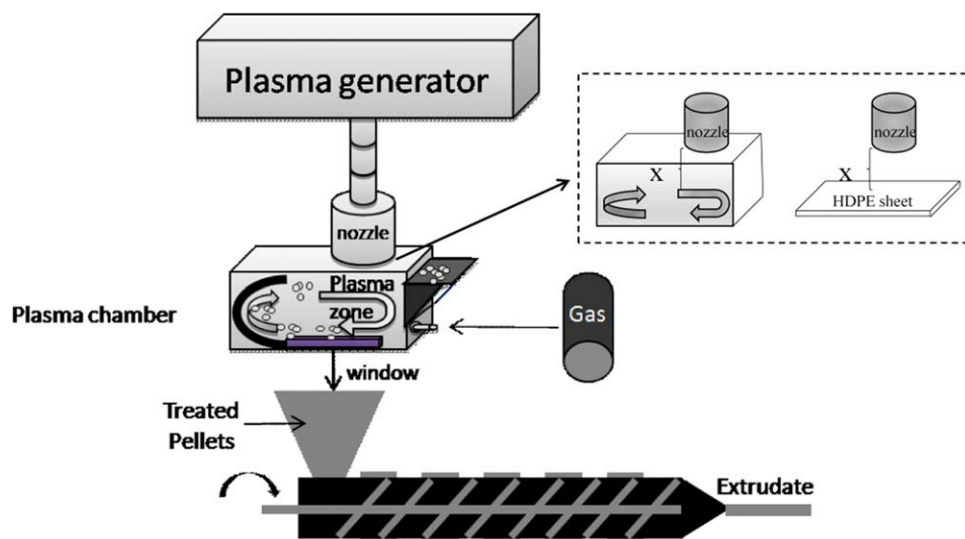


Figure 1. Schematic of the in-line plasma treatment process: pellets were treated in the plasma chamber and then passed through the feeding zone of the extruder. [Color figure can be viewed in the online issue, which is available at wileyonlinelibrary.com.]

treated polymers are altered in both chemical and molecular structures,¹⁵ the plasma modification only improves the hydrophilicity of polymers at polymer surfaces. The mild and fragile plasma treatment should be captured if the surface-treated fragments could be transferred into the bulk.

Therefore, in this study, the plasma treatment was applied on the plastic pellets in a fluidized box for a certain treatment time and then the treated pellets were immediately fed to the extruder in order to allow molecular flow so that those treated polar species occurred on the surface could be moved and entrapped inside the bulk polymer before they were evanescent as usual after aging; this technique is then called “pellet treatment.” This new application of plasma treatment is expected to gain benefits such as high energy irradiation but at lower cost and less process complication. Moreover, it can be viewed as a physical reactive extrusion to functionalize polymers where plasma-generated radicals replace the typical chemical initiators. This becomes a green process due to less use of chemicals. For the beginning of this approach using the nitrogen–air plasma, we would like to demonstrate this new application in comparison with the conventional plasma treatment in typical polymer process; i.e., in the step of surface coating or printing, the so-called “surface treatment,” where plasma treatment is performed on the surface of a plastic sheet. Generally, it is usually used to improve surface energy of HDPE from approximately 33 mJ m^{-2} to suitable level for adhesion to water-based adhesive ($44\text{--}50 \text{ mJ m}^{-2}$) or printing ($54\text{--}56 \text{ mJ m}^{-2}$).¹⁶ The effect of plasma treatment time on surface properties and chemical structure of treated samples were examined by contact angle measurement, attenuated total reflection-Fourier transform infrared spectroscopy (ATR-FTIR), and X-ray photoelectron spectroscopy (XPS), respectively, while the bulk properties were evaluated by thermal analysis and mechanical properties.

EXPERIMENTAL

Materials

HDPE pellets (trade name H5480S) was sponsored from The Siam Cement Group (SCG), Thailand (diameter 0.54 mm, MFI

$0.8 \text{ g } 10^{-1} \text{ min}^{-1}$, density 0.954 g cm^{-3}). It was dried at 60°C before use. For surface treatment, HDPE pellets were compressed at 210°C , 10 N for 5 min to a rectangular sheet with a dimension of $2 \times 7 \text{ cm}^2$, and the thickness was 1 mm.

Plasma Modification Process

For usual surface treatment, a HDPE sheet was treated by a commercial plasma unit with a frequency of 10 kHz and an effective voltage of 6 kV using various treatment time (from 15 to 120 s), and the surface-treated samples were designated to T15S–T120S where the number referred to treatment time in seconds.

On the other hand, HDPE pellets were fed to a treatment chamber, circulated by the mixture of air and nitrogen gas and exposed to plasma irradiation at a given treatment time, shown schematically in Figure 1. Nitrogen gas was directly (99.99% purity) injected (at pressure of 1 bar) into the plasma chamber, and air was emitted from the nozzle of the plasma generator. The plasma treatment chamber was installed on the feeding zone of a twin-screw extruder (LabTech type LHFS1-271822 corotating; nonintermeshing twin screw extruder) with an L/D ratio of 44 and a screw diameter of 20 mm. They were molten, extruded, and cut into the treated HDPE pellets, which were designated to T15–T120 where the number referred to pretreatment time in seconds. The temperature profile of the extruder was 180, 180, 185, 185, 190, 190, 190, 195, 195, and 200°C from hopper to die, respectively, with a screw speed of 20 rpm. The above mentioned conditions allowed production of continuous extrudates from the batch-fed HDPE pellets.

It should be noted that the effectiveness of plasma treatment also depends on the distance from the nozzle to specimens.¹⁷ Therefore, the gap for surface treatment was controlled by the gap between plasma nozzle and flow path of pellets inside plasma chamber (given in insert in Figure 1).

Characterization

Optical Microscopy. Before optical micrograph (OM) images of all fresh samples were captured, the freshly treated samples were drawn a line by the Dyne Test Pens (POLYTEST 38-40 Blue Pen

from Jemmco, LLC) of specific surface energy of 38–40 mN m⁻¹. The dyne pen was conducted parallel to the ASTM D2578. The OM images were captured by Leica optical microscopy model DM RXP using the magnification of four times for objective lens and 10 times for the camera. The observation was done both on treated surfaces and cross-sections of the test specimens.

Water Contact Angle Measurement. Pellet treatment samples were hot compressed under pressure of 10 N (similar condition for sheet preparation such as the sheet treatment samples) into a rectangular sheet. Hydrophilicity of the compression-molded pellet treatment samples (T15–T120) and surface treatment samples (T15S–T120S) was evaluated by averaging the measured contact angles of pure water droplets formed from a microsyringe onto the sample surface (at least five different areas), using a contact angle instrument (KRUSS G 10), at room temperature. The quoted results were the mean values of measurements on all droplets.

Attenuated Total Reflection–Fourier Transform Infrared Spectroscopy (ATR–FTIR). The functional groups on the surfaces of all specimens were analyzed using ATR-FTIR spectroscopy with a ZnSe crystal having a refractive index of 2.4, at incident angle θ of 45° equivalent to penetration depth 2 μ m. A Nicolet NEXUS 870 FTIR spectrometer with ATR attachment from Spectra Tech was used. The spectral range observed was 650–4000 cm⁻¹, and spectra were averaged over 64 scans for all samples.

X-ray Photoelectron Spectroscopy (XPS). Both qualitative and quantitative analysis of all specimens were examined by XPS (Kratos axis ultra DLD model) with a monochromatic X-ray source (Al K_{2s} anode). The base pressure during experiments was 3 × 10⁻⁹ Torr, and analyzed area was 700 × 300 μ m². Pass energy of 160 eV was used for wide scan in order to get percentage of atomic concentration of C1s, O1s, and N1s compositions. Moreover, for quantitative analysis, narrow scan with pass energy 40 eV was used for C1s, O1s, and N1s spectra. Then, all the spectra were referenced to the aliphatic C1s peak at 285.0 eV.

Gel Content. All samples were dissolved in xylene by using Soxhlet extraction apparatus from VELP Scientifica, model SER148 solvent extractor, at temperature of the heating plate of 210°C for 24 h to remove PE chains. Dry weight was measured for both before (W_i) and after Soxhlet extraction (W_f). Gel content of all sample was calculated following the equation:

$$\% \text{ Gel content} = \frac{W_f}{W_i} \times 100 \quad (1)$$

Differential Scanning Calorimetry (DSC). Nonisothermal of all samples was characterized by DSC, Mettler-Toledo DSC822, to investigate degree of crystallinity, melt temperature (T_m), and time that sample needs for crystallization. All DSC analyses were performed under dry nitrogen atmosphere. Sample was heated from 30°C at a heating rate of 40°C min⁻¹ to a fixed melt-annealing temperature of 200°C for 2 min in order to ensure complete melting. Then, each sample was cooled at constant cooling rate of 5 and 10°C min⁻¹ to 30°C.

Thermogravimetric Analysis (TGA). TGA analysis was performed with a TA Instruments TGA 2950 over a temperature

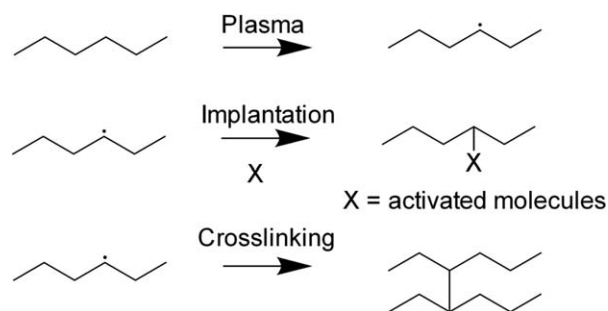


Figure 2. Schematic diagram of possible reactions by plasma treatment onto HDPE.

range 30–600°C at a heating rate of 10°C min⁻¹ under N₂ atmosphere. The activation energy for thermal decomposition (E_a) could be calculated from TGA thermograms by the Horowitz–Metzger integral kinetic method as follows^{18,19}:

$$\ln [\ln (1 - \alpha)^{-1}] = E_a \theta / RT_{dm}^2 \quad (2)$$

where α is the weight loss; E_a the activation energy for thermal decomposition; T_{dm} the temperature at the maximum rate of weight loss; θ the variable auxiliary temperature defined as $\theta = T - T_{dm}$, and R the universal gas constant. The E_a value can be estimated from the slope of a plot of $\ln [\ln (1 - \alpha)^{-1}]$ versus $\theta/R(T_{dm})^2$.

Tensile Properties. Tensile properties of all the plasma treatment samples were determined by using Universal Testing Machine (Instron) Model 33R4206, following ASTM D638 with the crosshead speed of 100 mm min⁻¹. The type 2 dumbbell specimens were cut from the sample sheets. The error bar was calculated from five repeating specimens for each sample.

RESULTS AND DISCUSSION

Plasma Reactions

Once plasma gas molecules and polymer surfaces expose to plasma radiation, free radicals and excited molecules can be generated.^{11,20} As shown in Figure 2, there are many possible reactions occurred via radicals during plasma treatment. After the subtraction of hydrogen atom from HDPE main chain by plasma treatment, implantation of HDPE could be occurred since the radical chains were combined by small activated molecules in the nitrogen and air mixture system. As found in the literature,^{11,21} during nitrogen plasma treatment, many active species of nitrogen atoms were generated, for example, NH^{*}, N₂^{*}, and N₂⁺. In addition, air from the nozzle of the commercial plasma was mixed with nitrogen gas; the nitrogen- and oxygen-containing functionalities are expected to implant onto polymeric surface.^{16,22–24} Another reaction was chain combination or crosslinking to create branch and network structures.²⁰ Especially, crosslinked structure was found to generate after modification of HDPE by plasma treatment, and it helped HDPE from rigorously susceptible hydrophobic-recovery when compared with other polyolefin treatments as reported by Tompkins *et al.*²⁵

Gel Content

As shown in Figure 3, gel content is found in both the plasma-treated samples; there are more gel content found in pellet

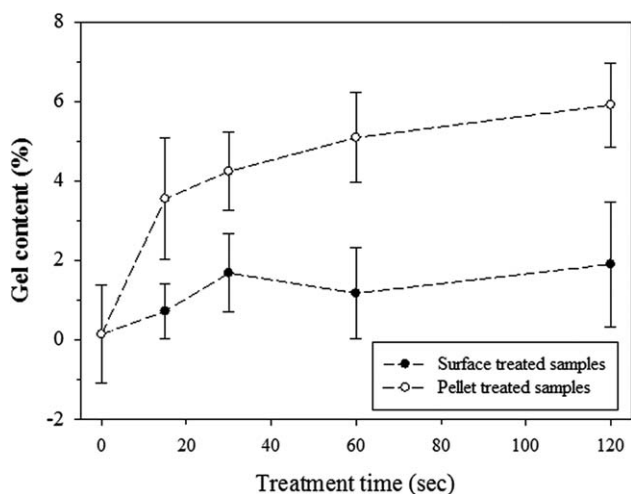


Figure 3. Gel content of surface-treated samples (—•) and pellet-treated samples (---○) with treatment time.

treatment (3.5–5.5 wt %) than in surface treatment (0.5 wt % to a steady value of about 1 wt % at 30 s and longer treatment time) with increasing treating times. The polymeric chain cross-linking is occurred during plasma treatment because plasma generates macroradicals, which interacts to each other by combination to terminate the radicals.^{4,6} After Soxhlet extraction with xylene at high temperature, the linear aliphatic polymer chains are certainly removed while the remaining part is the crosslinked polymer. From this result, gel content of the surface treatment is insignificant due to the reaction taking place only in the confined surface layer where limited number of radicals is produced.^{4,6,26} For pellet treatment, the free radicals were first generated on the pellet surface; then, the treated pellets were molten and sheared in the extruder at relatively high temperature so that the radicals are rather reactive to continue its reaction and create active species. It had more opportunities to confront with the surrounded polymer chains so that greater reactions occurred all over bulk polymer to produce partly crosslinked structure. It was also found by Kim *et al.*²⁷ that gel content increased to 10% after plasma modification to PE surface due to crosslinked structure. These high-order structures retard the flow and obstruct the segregation of hydrophilic species to the surface. For pellet treatment, increasing treatment time gradually creates more gel, and, thus, less hydrophilic surface is obtained.

Optical Micrograph

After plasma modification by both methods, a quick test for surface energy changing was done by using a dyne pen with surface energy of 38–40 mN m⁻¹. The smoothly continuous covering of the dye refers to the wettability improvement and also surface energy improvement, after plasma treatment, and the results are shown in Figure 4. From the figure, the dyne ink cannot spread over an untreated sample (T0) surface but becomes tiny droplets on specimen's surface indicating the lower surface energy of this treated surface than the test ink. In contrast to surface-treated samples, dyne ink is almost covered all surface even the shortest treatment time (T15S) and is completely covered (dark area) for longer treatment time (T30S–

T120S). Meanwhile, pellet treatment samples (T15–T120) show most areas covered by the dyne ink (the darkest area in T15 but less when treatment time increase for T30–T120). First, the results indicated the wettability and surface energy improvement on their surfaces after plasma modification and less when treatment time increased for pellet treatment method.

Moreover, for pellet treatment, the hydrophilic modified chains first generated on the surface could flow throughout the amorphous melt and the radical reaction could be occurred along reactive extrusion. A quick dyne test was done inside bulk polymer by marking on the cross-section surfaces of all samples. As expected, OM cross-section images of the surface treatment samples (T15S-x to T120S-x) showed most uncovered area and the small dyne droplets as untreated sample (T0-x), while pellet treatment (T15-x to T120-x) showed some parts smoothly covered by the dyne ink. From this result, it can be proved that wettability of HDPE pellet could be enhanced not only on its surface but also in the bulk polymer by plasma pretreatment together with reactive extrusion. In other words, this new application of plasma treatment on HDPE can alter the position of those hydrophilic species that are responsible for improved wettability of HDPE on the surface to be preserved inside the bulk polymer.

Contact Angle

Figure 5 reveals the contact angle value, which is a surface property measured from sessile drop testing. All plasma treatment samples exhibits lower water contact angle values than untreated sample (T0), confirming the improved hydrophilicity of the plasma-treated HDPE. From the results, water contact angle of surface treatment samples shows an extreme decrease from 96.8° to 49.5° after short treatment time (15 s) and gradually lowers to 43.6° for 120 s treatment time. The same findings have been generally observed as shown in the previous literature^{28,29} where the reduction of contact angle values with treatment time was explained by an introduction of polar groups onto polymer surface.

For pellet treatment method, the contact angle changes much less than that of the surface treatment. Its change is also opposite to that found in typical surface treatment. After treatment for 15 s, the contact angle decreased to 80.8° and then gradually increased with time to finally 88.9° at 120 s treatment time. Since increasing treatment time yields more polar species on the surface as found from surface treatment,¹¹ the incorporation of melt extrusion to immediately process these treated pellets can effectively rearrange those polarities. The polarity rearrangement is thus attributed to the chain movement in melt stage resulting to allow the dispersion of plasma-generated radicals and polar groups from surface into bulk and induce any possible reactions or aggregates of these active species during extrusion to yield bulky molecules or crosslinked structure,³⁰ which are not easy to flow. Some polar groups then remain in the bulk and difficult to diffuse to the surface. Increasing treatment time encourages the explained mechanism, while at short treatment time, the number of polar groups are small and chance to form aggregates are small so that the polar species prefer to segregate to surface. Therefore, with increasing treatment time, the polar

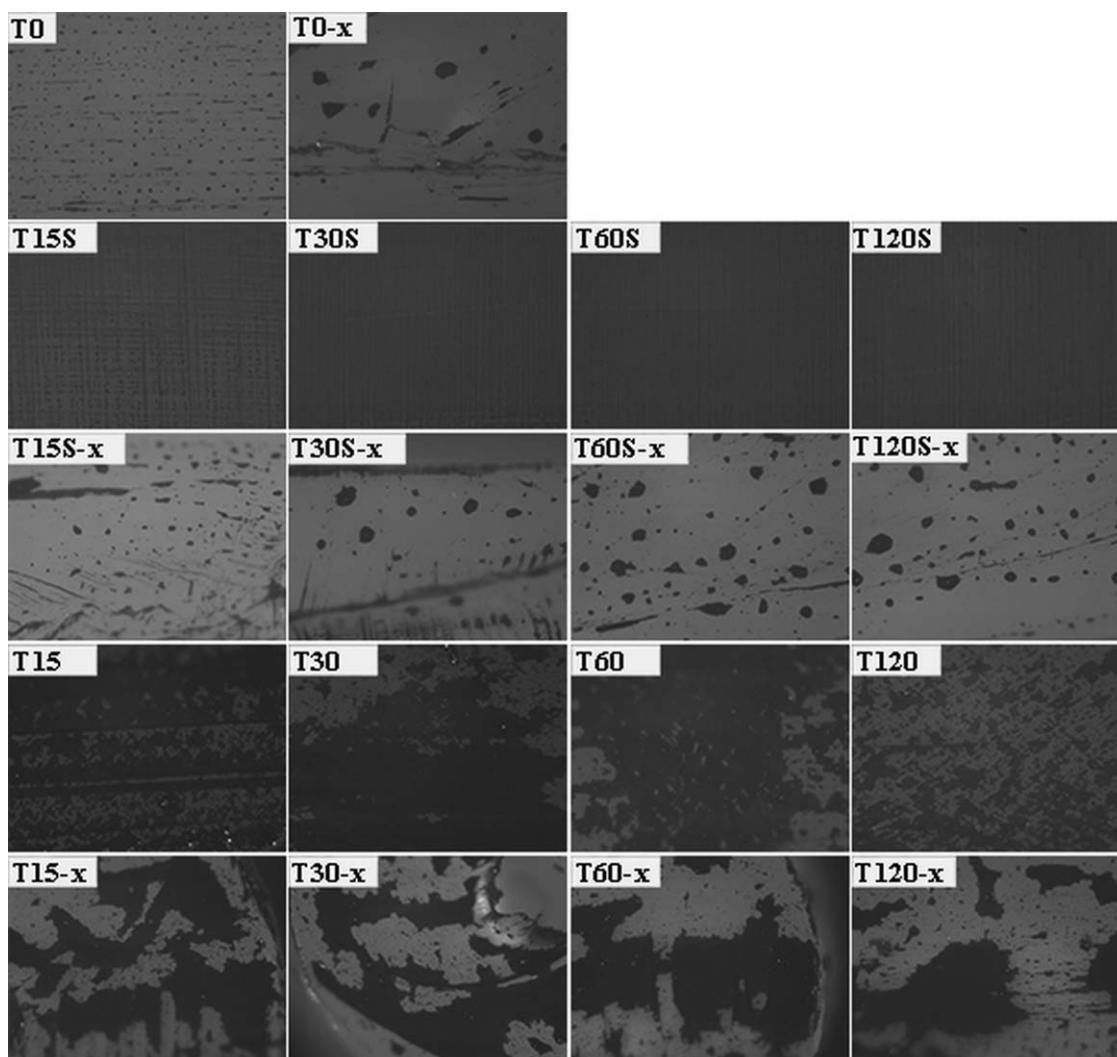


Figure 4. OM images of untreated sample (T0) covered by the dyne ink compared with those of the surface-treated samples (T15S–T120S) and pellet-treated samples (T15–T120); x refers to cross-section side of the specimens (dyne surface energy range 38–40 mN/m).

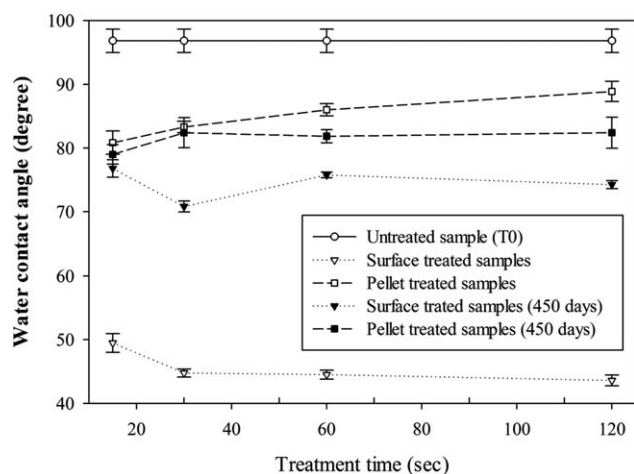


Figure 5. Water contact angle values of untreated sample (T0) (o), surface-treated samples before (∇) and after aging (▼), and pellet-treated samples before (□) and after aging (■) as a function of treatment time.

groups appear less on specimen's surface, and, so, the contact angle increases.

Hydrophobic recovery is well-known for plasma surface modification.^{9,30–32} After aging, all samples at 25°C and 50% relative humidity for 450 days, the water contact angle measurement was carried out again. As expected, in Figure 5, the surface-treated samples show obviously increasing contact angle values compared with those of their fresh samples. It is the result from diffusion process of low molecular weight oxidized species or the orientation of polar molecules on the surface into the bulk.³² Surprisingly, pellet-treated samples retain their surface hydrophilicity. The sample of long treatment time (120 s) showed less decrease in contact angle values. It could be explained again that the developed crosslinked structure in pellet-treated samples inhibits chain mobility and rearrangements of polar functional groups.^{25,31,32}

ATR-FTIR

ATR-FTIR was done to qualitatively investigate the chemical change on specimen's surface due to plasma treatment. Figures 6

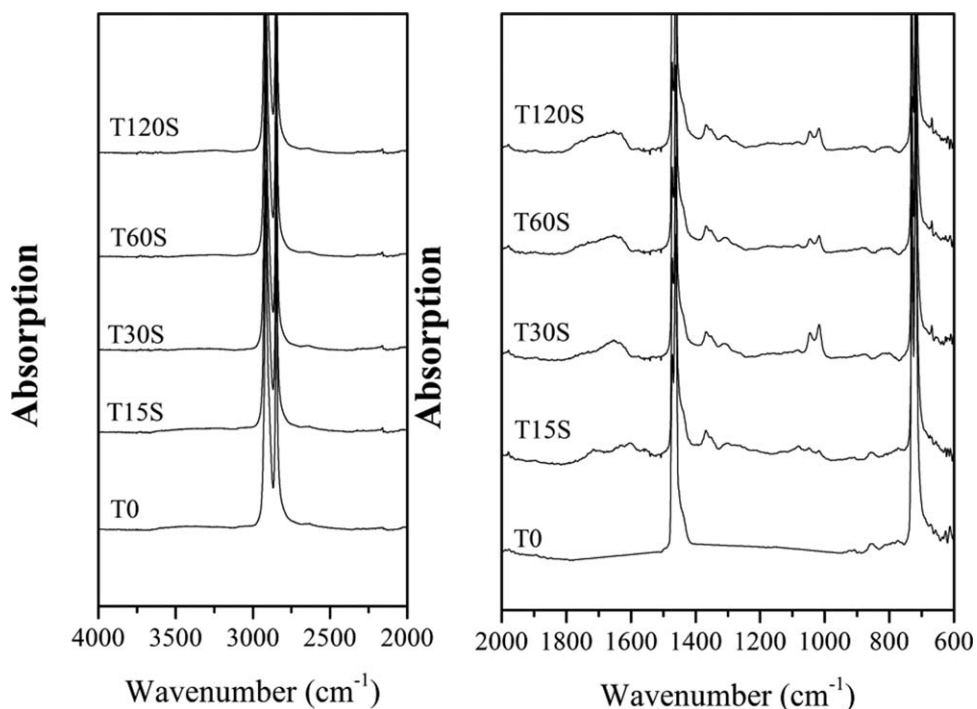


Figure 6. ATR-FTIR spectra of an untreated (T0) and the surface-treated samples at different treatment time.

and 7 show ATR-FTIR spectra of the surface-treated sheets and pellet-treated extrudates for wavenumber ranging from 4000 to 650 cm^{-1} , respectively. According to mixed plasma gases of nitrogen and air, the nitrogen- and oxygen-containing functionalities are expected to observe.^{16,22,23} In addition, oxygen-containing

functionality is presumed to originate from post-plasma oxidation of the activated surface on exposure to air.^{21,33}

From ATR-FTIR spectra, clear differences can be found between an untreated (T0) and the treated samples for both surface

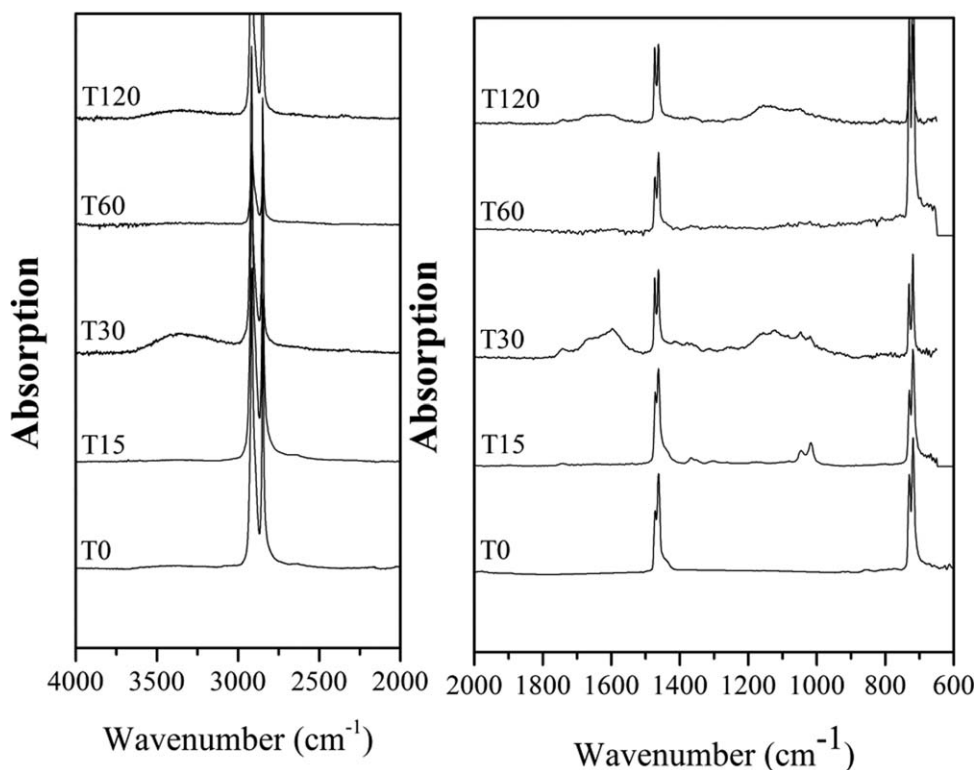


Figure 7. ATR-FTIR spectra of an untreated (T0) and the pellet-treated samples at different treatment time.

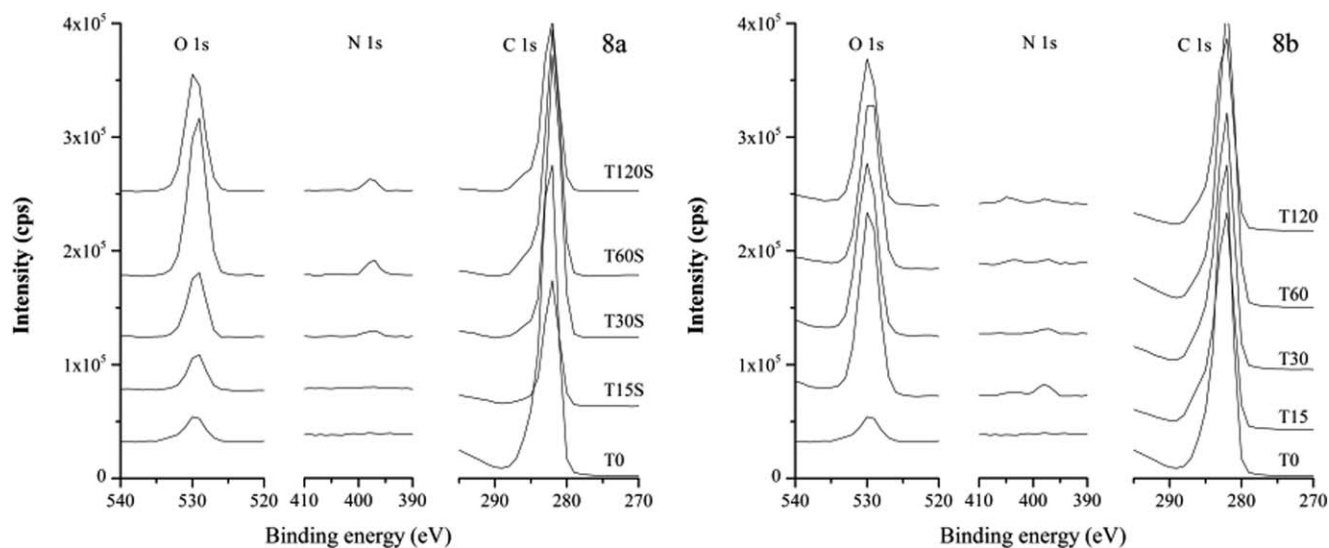


Figure 8. XPS wide scan spectra of surface-treated samples (a) and pellet-treated samples (b) at different treatment time (from 0 to 120 s).

treatment (T15S–T120S) and pellet treatment (T15–T120) samples in three regions. The new absorptions found only for the pellet-treated samples are in the following regions; first, a broad peak around $3000\text{--}3600\text{ cm}^{-1}$ for -OH and -NH stretchings, $1500\text{--}1750\text{ cm}^{-1}$ (especially at $1597\text{--}1631\text{ cm}^{-1}$) for COO- asymmetric stretching, or NH bending in amide or even C=N stretching in imine group as reported by Truica-Marasescu *et al.*²³ and 1743 cm^{-1} for -C=O stretching belonging to ketone, aldehyde, and carboxylic acid. The absorptions found mostly in the surface-treated samples are at wavenumber around $1014\text{--}1157\text{ cm}^{-1}$. These peaks can be attributed to C-N stretching in both primary and secondary amines and COO- symmetric stretching in oxygen-based group.

The possible presence of these functional groups containing nitrogen and oxygen are roughly estimated by ATR-FTIR absorption in order to point that plasma treatment leads to chemical change from fully hydrocarbon HDPE to hydrophilic-functionalized HDPE in accordance to the reduction in water contact angle values and the covering of dyne ink as shown earlier.

X-ray Photoelectron Spectroscopy

Results from XPS wide-scan analysis for changes in atomic content are shown in Figure 8 for surface treatment [Figure 8(a)] and pellets treatment [Figure 8(b)] samples in comparison with an untreated HDPE sample. The spectrum of the neat HDPE shows small amount of oxygen at binding energy around 532 eV, indicat-

ing that there are some oxidized contaminants in the starting material. After plasma treatment using nitrogen and air, XPS spectra from both the treatment methods show the new peaks appeared at 400 eV for nitrogen and at 532 eV for oxygen moieties where the latter peak intensity is considerably increased with increasing treatment time. Thus, the new polar groups are successfully introduced to hydrophobic HDPE polymer. Lastly, the shape of C1s peak at 285 eV is broaden to the higher binding energy; this is another evidence for some changes in chemical structure. The amount of introduced species was shown in Table I.

For the observed chemical change on surface, an untreated hydrophobic HDPE showed the original carbon and oxygen content of 96.5% and 3.5%, respectively. After plasma treatment, the oxygen content abruptly increased to about 30% for surface treatment and about 20% for pellet treatment. Similarly, the nitrogen content increased largely (4.6–6.7%) for surface treatment samples where the pellet treatment samples showed a significant increase in nitrogen content to 2% at 15 s treatment time but not at other longer treatment times (about 0.4%). This concentration is comparable with another experiment by Lee *et al.*,⁵ where they found that the nitrogen concentration increased from 0% to 2.3% after 5 min of nitrogen plasma onto PE surface. The chemical change on surface is thus pronounced in surface treatment samples rather than the pellet treatment samples. Moreover, increasing treatment time results in more chemical changes on surface for surface treatment samples but rather opposite for the pellet treatment samples

Table I. Percentage of Atomic Concentration (at %) on the Specimen's Surface after Different Plasma Treatment Condition

Atomic	Treatment time (s)									
	Surface treatment					Pellet treatment				
	0	15	30	60	120	0	15	30	60	120
C_s	96.55	65.76	62.46	69.17	62.39	96.55	74.5	78.74	81.09	77.59
O_s	3.45	29.68	32.21	26.08	30.87	3.45	23.47	20.48	18.33	21.98
N_s	0	4.56	5.33	4.76	6.73	0	2.02	0.79	0.58	0.43
$(\text{O+N})_s/\text{C}_s$	0.04	0.52	0.60	0.45	0.60	0.04	0.34	0.27	0.23	0.29

Table II. Percentage of Atomic Concentration (at %) Inside Bulk Polymer after Different Plasma Treatment Conditions

Atomic	Treatment time (s)									
	Surface treatment					Pellet treatment				
	0	15	30	60	120	0	15	30	60	120
C _b	95.84	96.45	95.34	94.87	96.58	95.84	78.33	75.48	89.64	81.41
O _b	4.16	3.55	4.66	5.13	3.42	4.16	18.72	23.01	9.91	17.43
N _b	0	0	0	0	0	0	2.95	1.51	0.44	1.16
(O+N) _b /C _b	0.04	0.04	0.05	0.05	0.04	0.04	0.28	0.32	0.12	0.23
O _s +O _b	7.61	33.23	36.87	31.21	34.29	7.61	42.19	43.49	28.24	39.41
N _s +N _b	0	4.56	5.33	4.76	6.73	0	4.97	2.3	1.02	1.59

where increasing treatment time rather decreases the chemical change on surface. Surface treatment results show the same situation as many studies^{11,16,28,33,34} that polar groups introduced by plasma treatment increased when treatment time increased in accordance to the decrease in contact angle values.

On the other hand, for the pellet treatment, all the treated pellets were fed into the reactive extruder; they were melted, mixed, and flowed along the extrusion. Their polar groups, originally introduced to polymer molecules on the pellet surface, were then dispersed freely in the dynamic flow, mixed, further interacted to each other in the melt, and, finally, rearranged themselves possibly inside and outside the extrudate strand. So, after the extrudate strand was cut into pellets, less polar groups come out on pellet's surface but more polar groups appear inside the pellets. Atomic concentrations of the polar groups in the bulk are determined as shown in Table II.

From Table II, nitrogen concentration investigated inside the bulk of the neat HDPE is none but oxygen content is about 4%. For surface treatment samples, oxygen content was not remarkable changed, and as expected, nitrogen atom was not observed because plasma treatment onto polymer surface does not affect to bulk polymer.³³ Although treatment time increases, the chemical contents in the bulk are hardly changed and similar to those of neat HDPE [see from the ratio of (O+N)_b/C_b, Table II]. The bulk part of the surface treatment samples is thus rather hydrophobic. On the others hand, oxygen concentration for pellet treatment was significantly enhanced from the original polymer (from about 4% to 10–23%). Especially, nitrogen concentration increases to about 3% at a short treatment time (15 s). The 30 s pellet treatment yields the highest oxygen content, and longer treatment time seems to lower both oxygen and nitrogen contents.

In addition, the total polar groups generated by pellet treatment method shows higher value than that of the surface treatment method. Moreover, for pellet treatment, the total polar group concentrations was achieved (about 42% for oxygen and 5% for nitrogen) when using 15 s plasma treatment. Meanwhile, surface treatment shows the highest polar groups concentration at treatment time 30 s, which is about 37% for oxygen and 5% for nitrogen. Thus, implantation reactions of small molecules by pellet treatment could further occur inside the reactive extruder

under high shear rate and temperature, resulting in higher amount of polar groups than that of surface treatment method in which implantation took place only on its surface. This indicates that the introduction of polar groups to hydrophobic polymer not only onto its surface but also inside bulk polymer is achieved by the new technique of pellet treatment method.

In addition, the ratios of total polar groups (nitrogen and oxygen contents) to carbon content of the pellet treatment samples at specimen's surface [(O+N)_s/C_s in Table I] are about half those of the surface treatment samples in accordance to the contact angle results. For the pellet treatment samples, their ratios of total polar groups to carbon content on the surface, (O+N)_s/C_s in Table I, are comparable with those in the bulk, (O+N)_b/C_b in Table II. Interestingly, this ratio is high for short treatment time and, then, lower and increase again for another minute of treatment, revealing the dynamic of implementation instability.

For more advantages of plasma-treated samples, printability and adhesive property are interested, as supported by the previous publications that the main factors for printability and adhesion with additives are oxygen and nitrogen contents.^{7,16} It was reported by López-García *et al.*⁷ that, after air plasma modification, oxygen and nitrogen contents were 20 and 5 at %, respectively, which correlated to contact angle around 60°. Therefore, from XPS and contact angle results, it can be implied in this work that printability and adhesive property of surface-treated samples (T15S–T120S) are improved and, for those of pellet-treated samples (T15–T120), are enhanced by the oxygen and nitrogen contents.

Qualitative analysis of the new chemical groups introduced by the mixture of nitrogen and air plasma treatment was examined by XPS narrow scan at specific binding energy. The result of pellet treatment showed the same trend of de-convolution peaks as example in Figure 9.

From Figure 9(a,b), three de-convoluted peaks of C1s were obtained on specimen surface and inside bulk polymer. These peaks contributed to carbon characteristic of C–C, C–O/C–N, and O–C=O^{5,11,35} at 285.0, 286.6, and 289.2 eV, respectively. Moreover, narrow scan at binding energy around 400 eV, which is the range of N1s atom, showed two de-convoluted peaks at 400.6 and 402.9 eV [Figure 9(c,d)]. According to the literature,^{24,34,36} there are many possible ways of nitrogen to bond with carbon during plasma treatment (amine, amide, imine, nitro, nitrate,

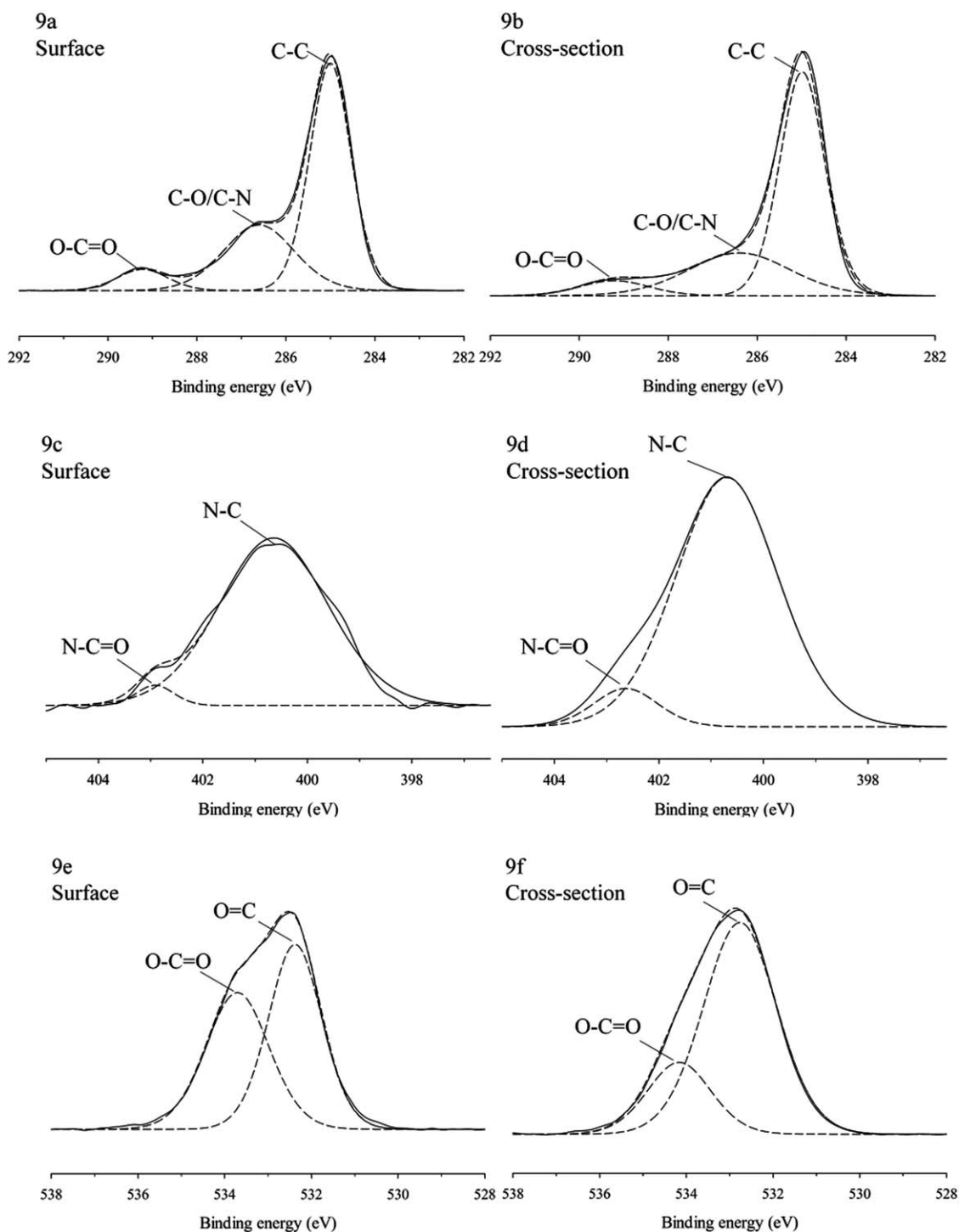


Figure 9. XPS narrow scan of C1s (a and b), N1s (c and d), and O1s (e and f) of pellet treatment at 15 s.

etc.). But, some functional groups, which nitrogen formed double bond to other atoms such as imine, nitro, and nitrate, were excluded because they should appear at high binding energy around 406–408 eV.³⁷ Therefore, new nitrogen-containing functionalities can be amine and amide groups at binding energies 400.6 and 402.9 eV, respectively. There are two components of oxygen atom, which are C=O and O–C=O at 532.4 and 533.1 eV^{3,29} [Figure 9(e,f)], respectively. XPS results further confirm the

ATR-FTIR analysis that the majority of nitrogen was implemented on pellet-treated HDPE as C–N group while oxygen as carbonyl group, C=O. The percentage of each functional group is shown in Table III for specimen's surface and Table IV for bulk polymer.

Differential Scanning Calorimetry

DCS measurement was done to study the thermal property of the samples including melting temperature and %crystallinity

Table III. Percentage of Functionality of Plasma Treatment Samples Observed onto Specimen's Surface

Samples	Binding energy (eV)						
	C1s			N1s		O1s	
	C—C	C—O/C—N	O—C=O	N—C	N—C=O	O=C	O=C—O
T0	94.2	5.8	0	0	0	100	0
T15S	56.4	9.3	34.3	59.8	40.2	71.9	28.1
T30S	65.4	24.5	10.1	68.7	31.3	98.1	1.9
T60S	68.9	18.6	12.6	64.7	35.3	96.4	3.6
T120S	65.7	17	17.3	68.6	31.4	92.4	7.6
T15	54.4	34.8	10.8	71.9	28.1	74.3	25.7
T30	62.1	30.8	7.1	96	4	53.3	46.7
T60	62.6	32.3	5.1	97	3	70	30
T120	52.1	40.6	7.2	92.9	7.1	57.8	42.2

Table IV. Percentage of Functionality of Plasma Treatment Samples Observed inside Bulk Polymer

Samples	Binding energy (eV)						
	C1s			N1s		O1s	
	C—C	C—O/C—N	O—C=O	N—C	N—C=O	O=C	O=C—O
T0	94	6	0	0	0	100	0
T15S	92.7	5.4	1.9	0	0	98.1	1.9
T30S	93.8	4.8	1.4	0	0	81.4	18.6
T60S	85	13.8	1.2	0	0	79.9	20.1
T120S	75	21.4	3.6	0	0	68	32
T15	60.2	28.4	11.4	76.7	23.3	82.9	17.1
T30	65	28.3	6.7	91.2	8.8	77.2	22.8
T60	75.5	18.5	6	79.5	20.5	55.4	44.6
T120	57.1	30.2	12.8	89.7	10.3	70.2	29.8

(χ_c) of all plasma treatment samples compared with untreated sample. The results are listed in Table V. From the peak melting temperature, T_m , there is a slight decrease of 1–2°C from T_m of HDPE. It is in accordance with other reports^{28,38,39} that they did not find the change in melting temperature after plasma modification. However, degree of crystallinity was observed to decrease from 76% in untreated sample (T0) to 69–63% in

plasma treatment samples. As mentioned earlier, because, during plasma treatment, polar groups or bulky structure could be formed, it obstructed the packing of polymer chains or the crystallization process. In addition, degree of crystallinity was affected by implantation of plasma gases. The more polar groups implanted the less degree of crystallinity (see details in Table II and Table V). Banik *et al.*⁴⁰ observed that the degree of

Table V. List of Time for Crystallization ($t_{1/2}$ and t_{end}), Melting Temperature (T_m), and Degree of Crystallinity (χ_c) From DSC Measurement and Maximum Decomposition Temperature (T_{dm}) From TGA Measurement

Treatment time (s)	Surface treatment					Pellet treatment				
	$t_{1/2}$ (min)	t_{end} (min)	T_m^a (°C)	χ_c^a (%)	T_{dm} (°C)	$t_{1/2}$ (min)	t_{end} (min)	T_m^a (°C)	χ_c^a (%)	T_{dm} (°C)
0	0.69	8.48	132.17	75.71	451.74	0.69	8.48	132.17	75.71	451.74
15	0.92	11.72	131.90	67.49	453.15	0.81	10.60	130.49	66.08	453.29
30	0.77	11.72	131.54	68.54	458.75	0.58	10.79	130.78	63.15	453.78
60	0.71	11.20	132.54	68.85	464.77	0.53	10.30	130.50	62.74	465.82
120	0.89	11.32	132.02	68.3	461.92	0.53	12.60	131.08	63.96	466.64

^a At heating rate 10°C/min.

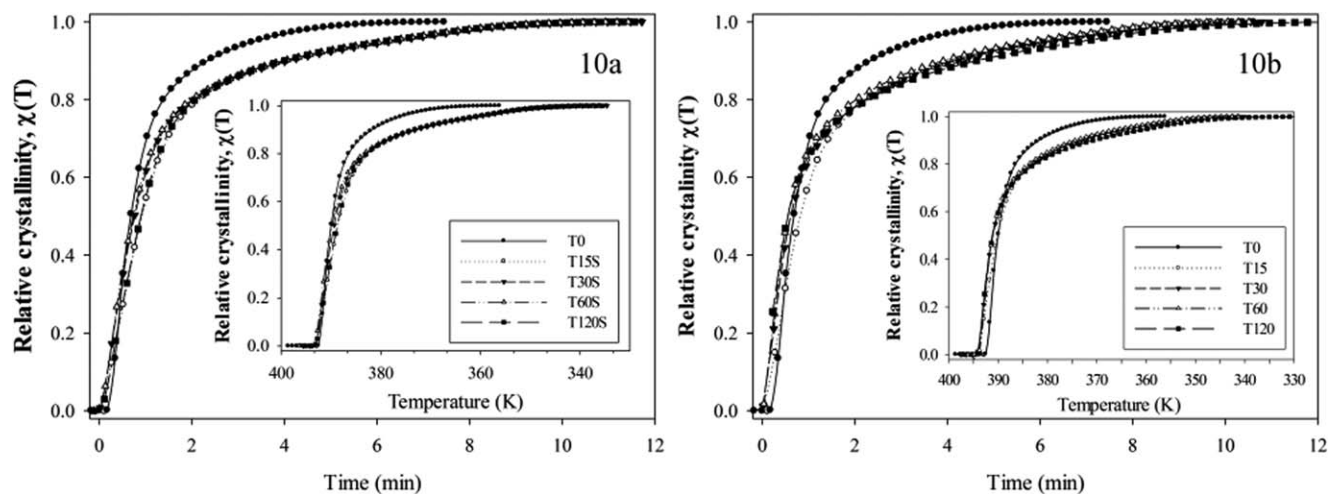


Figure 10. Crystallization behavior of untreated samples (T0), surface-treated samples (T15S–T120S; (a) and pellet-treated samples (T15–T120; (b)).

crystallinity decreased with oxygenation reaction during oxygen plasma treatment onto HDPE surfaces. Indeed, plasma treatment on plastic pellets coupled with reactive extrusion showed lower degree of crystallinity than the surface treatment because of more implantation of active polar groups during reactive extrusion as described in XPS part. Besides, the crosslink structure was formed as seen by increasing gel content (Figure 3) and could obstruct the crystallization. Alvarez *et al.*³⁹ found that, after plasma treatment, crystallization process was delayed due to crosslinked structure. However, the gel content in the surface treatment samples was much smaller than that in pellet treatment. This contributed to rather high crystallinity of the surface treatment than the pellet treatment samples. In addition, it is clear that plasma treatment affects crystallization process of the modified samples; crystallization behavior of all samples was further investigated at cooling rate $5^{\circ}\text{C min}^{-1}$, as shown in Figure 10, which is the plot between relative degree of crystallinity, $\chi(T)$, with time for crystallization of polymer. The details including time for 50% of crystallization process ($t_{1/2}$) and time for complete crystallization process (t_{end}) are listed in Table V.

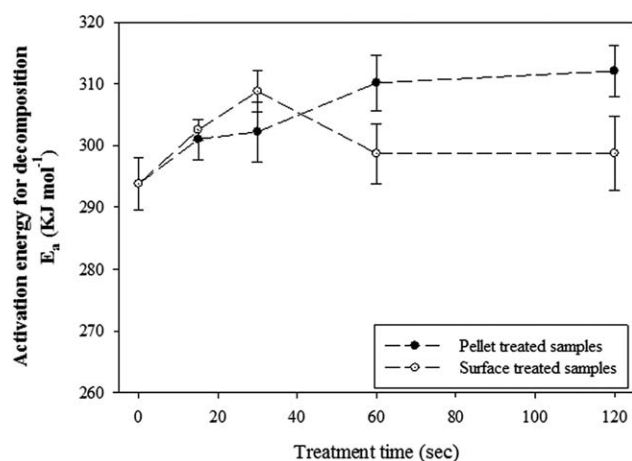


Figure 11. Activation energy for decomposition (E_a) of untreated (at treatment time = 0) compared with surface- (o) and pellet-treated (•) samples at different treatment time.

As compared with the untreated sample, the surface treatment samples show longer crystallization half time and total crystallization time. The effect of treatment time on the crystallization kinetics seems to be insignificant. For the pellet treatment samples, the crystallization half time for 15 s treated sample was longer than that of the neat HDPE and became shorter with increasing treatment time. The pellet treatment samples were crystallized at higher temperature than the neat HDPE, suggesting that the high gel content is strong enough to act as nucleating agent to facilitate crystallization and become obstacle for molecular packing so that the crystallization finishes at delayed time. Thus, the treatment method is more significant on crystallization kinetics than the treatment time. The gel content and the interaction of polar groups by plasma treatment on pellet plus reactive extrusion play strong role in crystallization and crystallinity of HDPE rather than those generated by surface treatment.

Activation Energy for Decomposition

Figure 11 compares values of activation energy (E_a) for decomposition determined by TGA measurement for all HDPE-treated samples. Plasma-treated samples show extended decomposition temperature, which confirms the presence of polar implantation and crosslinked structure that provide high intermolecular bonding. The results of pellet treatment samples showed more retarded decomposition from those of untreated sample and surface treatment samples. It concludes that the polar groups induce higher interaction between polymer chains, which is not only van der Waal force but also dipole–dipole interaction. Moreover, the crosslinking to produce network structure also contributes to the high intermolecular force. For pellet treatment samples, they showed an increment of E_a after plasma treatment, and E_a was further increased when treatment time increased. E_a values of both the treatment samples are comparable at low treatment time (15–30 s) although the pellet treatment samples seem to have slightly lower values. For 60- and 120-s treatment time, E_a values of the pellet treatment samples were larger than those of the surface treatment samples. It is noted that E_a values of the surface treatment samples are rather similar to that value of the neat HDPE except the one treated at 30 s, which shows higher values than the others due to more

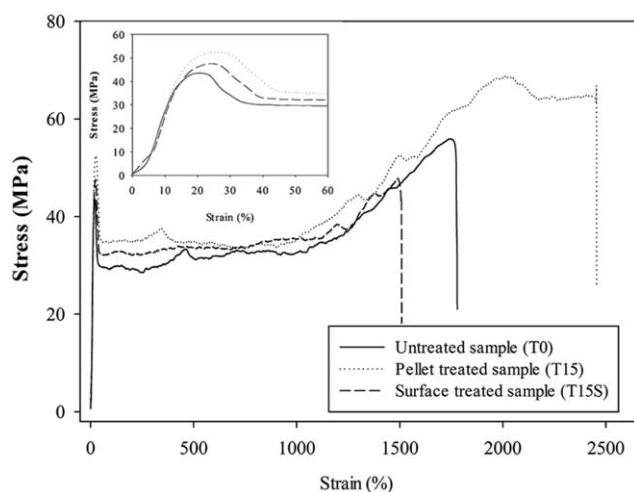


Figure 12. Stress–strain curve of untreated (T0) compared with pellet-treated (T15) and surface-treated (T15S) samples at 15 s of treatment time.

interaction from the highest content of polar groups. This is well-known that surface treatment does not affect bulk property of the polymer.³³ It is further discussed that by pellet treatment: the increasing treatment time does not show much effect on increasing polar groups but significantly increase in gel content and E_a or thermal decomposition temperature. This informs that the plasma treatment not only implement the polar groups but also generate free radicals that are responsible for forming branch or crosslink structure, and the radicals still performed well in the hot extrusion to yield network structure. The longer the treatment time produced the more active radicals. By pellet treatment, both implantation and crosslinked reaction can further take place along the reactive extrusion resulting in higher polar group concentrations with well distributed throughout the mass of sample and crosslinked structure inside or in the bulk polymer. The results agree with the XPS, gel content, and DSC results. Consequently, HDPE that is treated by this novel pellet treatment method becomes more polar (as bulk property not only on the surface) with better thermally stability and possibly stronger than usual. In practice, this treated HDPE should be reprocessable or recycled without much chain degradation. Moreover, with the improvement in polarity, this treated HDPE is then better compatible with other polymers.

Tensile Properties

Tensile properties of all plasma treatment samples were determined to confirm the improvement of bulk property due to structural change. As in Figure 12, examples of stress–strain curves were plotted for untreated sample (T0) and surface- and pellet-treated samples at 15 s of treatment time. All samples show the ductile behavior of PE. It contains the strong yielding peak at low strain, necking at medium strain, and strain hardening before breaking at high strain.

It is well-known that surface plasma modification on polymer sheet yields chemical and structural changes to only a few micrometer in depth as reported in many previous researches.^{4,22,34} Therefore, bulk property, including thermal property, of the surface-treated samples does not change significantly. From Table VI, Young's modulus of the surface-treated sample is comparable with that of the untreated sample at 470 MPa, while for that of the pellet-treated sample, a significant increase in Young's modulus to 517 MPa is obtained after short treatment time (15 s) due to the introduced crosslinked structure as evident by the gel result. In other words, the HDPE structural change from linear chains to partly crosslinked structure in the pellet-treated samples is ensured. Moreover, Young's modulus tends to increase slowly with treatment time in accordance to a gradual increase in gel content (3.5–5.5%; Figure 13).

The presence of crosslinked structure also affects to yield strength, which is one of the important properties because it can identify the maximum load that materials can resist to tension force without deformation. Again, surface-treated samples do not change significantly. Meanwhile, the pellet-treated samples show significant increase of yield strength from the untreated sample by 7–12%.

Moreover, pellet-treated samples exhibit large increase in tensile strength and elongation at break in comparison with those of untreated and surface-treated samples. It can be also explained by the crosslinked structure.⁴¹ After yield point, crystalline and crosslinked parts respond to tension by chain drawing and anti-chain slippage. However, crosslinked structure is the chemical linkage, which is stronger than physical interaction of crystal lamellar. It restricts the chain slippage resulting in high tensile strength. In addition, during plasma treatment, oxygen and nitrogen atoms were introduced into the bulk yielding high

Table VI. List of Mechanical Properties of Untreated (Treatment Time = 0), Pellet-Treated Samples, and Surface-Treated Samples

Treatment time (s)	Surface-treated samples				Pellet-treated samples			
	Modulus Young's (MPa)	Yield strength (MPa)	Tensile strength (MPa)	Elongation at break (mm/mm)	Modulus Young's (MPa)	Yield strength (MPa)	Tensile strength (MPa)	Elongation at break (mm/mm)
0	470.3 ± 23.5	42.3 ± 2.4	53.3 ± 3.2	17.3 ± 0.4	470.3 ± 23.5	42.3 ± 2.4	53.3 ± 3.2	17.3 ± 0.4
15	460.6 ± 28.2	44.2 ± 2.5	59.0 ± 4.2	15.1 ± 3.6	517.8 ± 11.6	47.6 ± 1.9	62.1 ± 7.2	24.7 ± 0.7
30	440.6 ± 12.5	43.0 ± 0.8	59.8 ± 6.9	21.3 ± 0.9	498.5 ± 29.6	45.1 ± 3.0	66.1 ± 4.3	27.7 ± 3.2
60	457.9 ± 38.6	40.2 ± 1.8	54.0 ± 5.4	18.2 ± 2.2	527.3 ± 35.0	45.2 ± 1.5	64.5 ± 2.1	25.7 ± 0.5
120	479.9 ± 15.8	38.5 ± 2.1	57.9 ± 8.7	18.5 ± 2.6	519.6 ± 41.7	45.3 ± 1.6	63.5 ± 3.9	25.3 ± 0.2

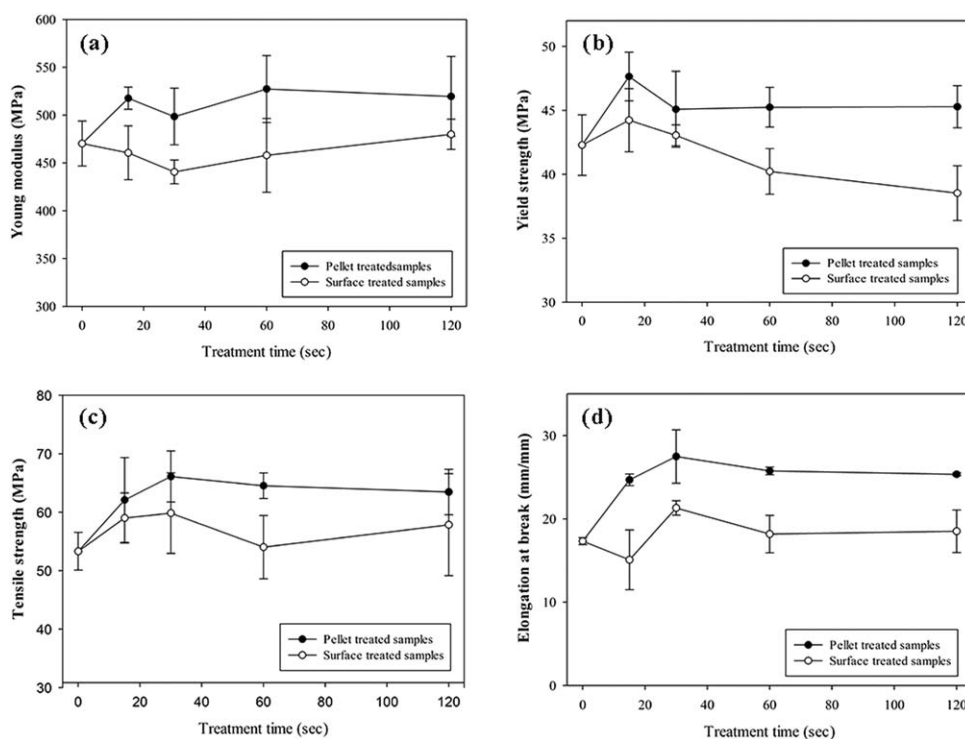


Figure 13. Young's modulus (a), yield strength (b), tensile strength (c), and elongation at break (d) of untreated sample compared with those of pellet- and surface-treated samples in the dependence of treatment time.

intermolecular force (from E_a for decomposition). It could enhance slippage restriction too.

CONCLUSIONS

With an aim to distribute the hydrophilicity caused by plasma treatment throughout the bulk of polymer, e.g., PE, a new technique called pellet treatment method is employed as a sequence of plasma treatment on pellets and reactive extrusion. By using nitrogen and air atmospheric plasma treatment, this work demonstrates clearly the differences caused by the novel pellet treatment method and the common plasma treatment on surface (of plastic objects, e.g., sheet), which is called the surface treatment method. The conventional surface treatment method yield only an intense in hydrophilicity due to the presence of oxygen- and nitrogen-containing species (mostly carbonyl and amine groups) on the surface as evidenced by sudden lowering of contact angle and high polar group content as shown by dyne test pen-OM testing, ATR-FTIR, and XPS. However, the chemical change in bulk property hardly occurred including crosslinking (about 1 wt % gel); so, the activation energy for thermal decomposition is not much affected. The hydrophilicity then affects to retard crystallization kinetic and lowering melting temperature and crystallinity. The optimum treatment time is about 30 s (37% and 5% of oxygen and nitrogen contents, respectively), and increasing treatment time does not significantly change the chemical and thermal properties.

On the other hand, the pellet treatment method employs the use of plasma treatment to provide those hydrophilicity and free radicals as reactive species for further reaction in the hot extrusion (reactive extrusion) and the use of melt extrusion to

distribute the hydrophilic implementation into the bulk and simultaneously allow the active radicals to form crosslinked network. The hydrophilicity is thus found quite evenly in both surface (with less amount or higher contact angle than that found in surface treatment method) and the bulk as clearly shown by dyne test pen-OM, ATR-FTIR, and XPS. The gel content is relatively high about 3.5–5.5 wt %. Moreover, the total polar group implementation is higher than that found in surface treatment. The optimum treatment time for high hydrophilicity (42% and 5% for oxygen and nitrogen contents, respectively) is 15 s, which is shorter than the surface treatment method. Increasing treatment time does not further enhance the hydrophilicity but prefers to form crosslinked structure, which is contributed to enhance thermal stability with higher decomposition temperature and activation energy than those obtained by surface treatment method. Moreover, pellet treatment method affects to retard the hydrophobic recovery; so, contact angle retains its fresh value after long aging. Interestingly, although the hydrophilicity and gel lower melting temperature and the crystallinity (less than those found by surface treatment method), the crystallization kinetics is found to be faster than those of common HDPE, suggesting that the gel structure is strong enough to perform as nucleating agent. As a result of hydrophilicity interaction and the developed crosslinked structure by pellet treatment method, the mechanical properties of the treated HDPE are obviously improved.

ACKNOWLEDGMENTS

Funding was provided by The Royal Golden Jubilee Ph.D. Program (RGJ-Ph.D.), Thailand.

REFERENCES

1. Morra, M.; Occhiello, E.; Garbassi, E. *J. Adhes. Sci. Technol.* **1993**, *7*, 1051.
2. Kaplan, S. L.; Rose, P. W. *Int. J. Adhes. Adhesives* **1991**, *11*, 109.
3. Chung, H. J.; Rhee, K. Y.; Han, B. S.; Ryu, Y. M. *J. Alloys Compd.* **2008**, *459*, 196.
4. Choi, D. M.; Park, C. K.; Cho, K.; Park, C. E. *Polymer* **1997**, *38*, 6243.
5. Lee, J. H.; Rhee, K. Y.; Lee, J. H. *Appl. Surf. Sci.* **2009**, *256*, 876.
6. Yao, Y.; Liu, X.; Zhu, Y. *J. Adhes. Sci. Technol.* **1993**, *7*, 63.
7. López-García, J.; Bílek, F.; Lehocký, M.; Junkar, I.; Mozetič, M.; Sowe, M. *Vacuum* **2013**, *95*, 43.
8. Lehocký, M.; Drnovská, H.; Lapčíková, B.; Barros-Timmons, A. M.; Trindade, T.; Zembala, M.; Lapčík, L. Jr. *Colloids Surf. A* **2003**, *222*, 125.
9. Van Deynse, A.; Cools, P.; Leys, C.; Morent, R.; De Geyter, N. *Surf. Coat. Technol.* **2014**, *258*, 359.
10. Arpagaus, C.; Rossi, A.; Rudolf von Rohr, P. *Appl. Surf. Sci.* **2005**, *252*, 1581.
11. Bretagnol, F.; Tatoulian, M.; Arefi-Khonsari, F.; Lorang, G.; Amouroux, J. *React. Funct. Polym.* **2004**, *61*, 221.
12. Meyer-Plath, A. A.; Finke, B.; Schröder, K.; Ohl, A. *Surf. Coat. Technol.* **2003**, *174–175*, 877.
13. Hegemann, D.; Brunner, H.; Oehr, C. *Nucl. Instrum. Methods Phys. Res. Sect. A* **2003**, *208*, 281.
14. Xiao-Jing, L.; Guan-Jun, Q.; Jie-Rong, C. *Appl. Surf. Sci.* **2008**, *254*, 6568.
15. Burillo, G.; Clough, R. L.; Czvikovszky, T.; Guven, O.; Le Moel, A.; Liu, W.; Singh, A.; Yang, J.; Zaharescu, T. *Radiat. Phys. Chem.* **2002**, *64*, 41.
16. De Geyter, N.; Morent, R.; Leys, C. *Surf. Interface Anal.* **2008**, *40*, 608.
17. Gao, Z. *Appl. Surf. Sci.* **2011**, *257*, 2531.
18. Horowitz, H. H.; Metzger, G. *Anal. Chem.* **1963**, *35*, 1464.
19. Kim, J. Y.; Kim, D. K.; Kim, S. H. *Eur. Polym. J.* **2009**, *45*, 316.
20. Pankaj, S. K.; Bueno-Ferrer, C.; Misra, N. N.; Milosavljević, V.; O'Donnell, C. P.; Bourke, P.; Keener, K. M.; Cullen, P. J. *Trends Food Sci. Technol.* **2014**, *35*, 5.
21. Sanchis, M. R.; Calvo, O.; Fenollar, O.; Garcia, D.; Balart, R. *Polym. Test.* **2008**, *27*, 75.
22. Morent, R.; De Geyter, N.; Leys, C.; Gengembre, L.; Payen, E. *Surf. Interface Anal.* **2008**, *40*, 597.
23. Truica-Marasescu, F.; Girard-Lauriault, P. L.; Lippitz, A.; Unger, W. E. S.; Wertheimer, M. R. *Thin Solid Films* **2008**, *516*, 7406.
24. Foerch, R.; McIntyre, N. S.; Sodhi, R. N. S.; Hunter, D. H. *J. Appl. Polym. Sci.* **1990**, *40*, 1903.
25. Tompkins, B. D.; Fisher, E. R. *J. Appl. Polym. Sci.* **2015**, *132*, 41978.
26. Hudis, M. *J. Appl. Polym. Sci.* **1972**, *16*, 2397.
27. Kim, B. K.; Kim, K. S.; Park, C. E.; Ryu, C. M. *J. Adhes. Sci. Technol.* **2002**, *16*, 509.
28. Sanchis, M. R.; Blanes, V.; Blanes, M.; Garcia, D.; Balart, R. *Eur. Polym. J.* **2006**, *42*, 1558.
29. Ren, C. S.; Wang, K.; Nie, Q. Y.; Wang, D. Z.; Guo, S. H. *Appl. Surf. Sci.* **2008**, *255*, 3421.
30. Švorčík, V.; Kotál, V.; Slepíčka, P.; Bláhová, O.; Špírková, M.; Sajdl, P.; Hnatowicz, V. *Nucl. Instrum. Methods Phys. Res. Sect. A* **2006**, *244*, 365.
31. Ren, Y.; Wang, C.; Qiu, Y. *Surf. Coat. Technol.* **2008**, *202*, 2670.
32. Švorčík, V.; Kolářová, K.; Slepíčka, P.; Macková, A.; Novotná, M.; Hnatowicz, V. *Polym. Degrad. Stab.* **2006**, *91*, 1219.
33. Guruvenket, S.; Rao, G. M.; Komath, M.; Raichur, A. M. *Appl. Surf. Sci.* **2004**, *236*, 278.
34. Vesel, A.; Junkar, I.; Cvelbar, U.; Kovac, J.; Mozetic, M. *Surf. Interface Anal.* **2008**, *40*, 1444.
35. Liu, H.; Xie, D.; Qian, L.; Deng, X.; Leng, Y. X.; Huang, N. *Surf. Coat. Technol.* **2011**, *205*, 2697.
36. Wang, Y.; Lu, L.; Zheng, Y.; Chen, X. *J. Biomed. Mater. Res A* **2006**, *76A*, 589.
37. Morent, R.; Geyter, N. D.; Gengembre, L.; Leys, C.; Payen, E.; Iierberghe, S. V.; Schacht, E. *Eur. Phys. J. Appl. Phys.* **2008**, *43*, 289.
38. Patra, N.; Hladik, J.; Pavlatová, M.; Militký, J.; Martinová, L. *Polym. Degrad. Stab.* **2013**, *98*, 1489.
39. Alvarez, V. A.; Perez, C. *J. Thermochim. Acta* **2013**, *570*, 64.
40. Banik, I.; Kim, K. S.; Yun, Y. I.; Kim, D. H.; Ryu, C. M.; Park, C. S.; Sur, G. S.; Park, C. E. *Polymer* **2003**, *44*, 1163.
41. Kuan, H. C.; Kuan, J. F.; Ma, C. C. M.; Huang, J. M. *J. Appl. Polym. Sci.* **2005**, *96*, 2383.